Reconciling lattice and continuum models for polymers at interfaces

ARTICLE *in* THE JOURNAL OF CHEMICAL PHYSICS · APRIL 2012

Impact Factor: 2.95 · DOI: 10.1063/1.3693515 · Source: PubMed

2 AUTHORS:

Gerard J Fleer
Wageningen University
206 PUBLICATIONS **8,242** CITATIONS
SEE PROFILE

Alexander M. Skvortsov
Chemical Pharmaceutical Academie . St.Pete…
152 PUBLICATIONS **1,670** CITATIONS
SEE PROFILE

Reconciling lattice and continuum models for polymers at interfaces

G. J. Fleer and A. M. Skvortsov

Citation: J. Chem. Phys. **136**, 134707 (2012); doi: 10.1063/1.3693515
View online: http://dx.doi.org/10.1063/1.3693515
View Table of Contents: http://jcp.aip.org/resource/1/JCPSA6/v136/i13
Published by the American Institute of Physics.

Reconciling lattice and continuum models for polymers at interfaces

G. J. Fleer[1] and A. M. Skvortsov[2]
[1]*Laboratory of Physical and Colloid Science, Wageningen University, 6703 HB Wageningen, The Netherlands*
[2]*Chemical-Pharmaceutical Academy, Prof Popova 14, 197022 St. Petersburg, Russia*

(Received 6 December 2011; accepted 22 February 2012; published online 5 April 2012)

It is well known that lattice and continuum descriptions for polymers at interfaces are, in principle, equivalent. In order to compare the two models quantitatively, one needs a relation between the inverse extrapolation length c as used in continuum theories and the lattice adsorption parameter $\Delta\chi_s$ (defined with respect to the critical point). So far, this has been done only for ideal chains with zero segment volume in extremely dilute solutions. The relation $\Delta\chi_s(c)$ is obtained by matching the boundary conditions in the two models. For depletion (positive c and $\Delta\chi_s$) the result is very simple: $\Delta\chi_s = \ln(1 + c/5)$. For adsorption (negative c and $\Delta\chi_s$) the ideal-chain treatment leads to an unrealistic divergence for strong adsorption: c decreases without bounds and the train volume fraction exceeds unity. This due to the fact that for ideal chains the volume filling cannot be accounted for. We extend the treatment to real chains with finite segment volume at finite concentrations, for both good and theta solvents. For depletion the volume filling is not important and the ideal-chain result $\Delta\chi_s = \ln(1 + c/5)$ is generally valid also for non-ideal chains, at any concentration, chain length, or solvency. Depletion profiles can be accurately described in terms of two length scales: $\rho = \tanh^2[(z + p)/\delta]$, where the depletion thickness (distal length) δ is a known function of chain length and polymer concentration, and the proximal length p is a known function of c (or $\Delta\chi_s$) and δ. For strong repulsion $p = 1/c$ (then the proximal length equals the extrapolation length), for weaker repulsion p depends also on chain length and polymer concentration (then p is smaller than $1/c$). In very dilute solutions we find quantitative agreement with previous analytical results for ideal chains, for any chain length, down to oligomers. In more concentrated solutions there is excellent agreement with numerical self-consistent depletion profiles, for both weak and strong repulsion, for any chain length, and for any solvency. For adsorption the volume filling dominates. As a result c now reaches a lower limit $c \approx -0.5$ (depending slightly on solvency). This limit follows immediately from the condition of a fully occupied train layer. Comparison with numerical SCF calculations corroborates that our analytical result is a good approximation. We suggest some simple methods to determine the interaction parameter (either c or $\Delta\chi_s$) from experiments. The relation $\Delta\chi_s(c)$ provides a quantitative connection between continuum and lattice theories, and enables the use of analytical continuum results to describe the adsorption (and stretching) of lattice chains of any chain length. For example, a fully analytical treatment of mechanical desorption of a polymer chain (including the temperature dependence and the phase transitions) is now feasible. © *2012 American Institute of Physics*. [http://dx.doi.org/10.1063/1.3693515]

I. INTRODUCTION

The behavior of polymers in a solution near a solid surface is an important topic in various areas of physics, chemistry, and biology. Applications of adsorption and depletion phenomena in polymer solutions can be found in such diverse fields as steric stabilization of colloidal particles,[1–3] flow injection,[4] drug delivery,[5] size-exclusion chromatography,[6] and membrane-polymer interactions.[7] Understanding such phenomena is also important for different applications in nanotechnology.[8]

On the mean-field level, numerical self-consistent field (SCF) lattice theory for a polymer solution next to an attractive or repulsive surface has greatly improved our understanding of polymer adsorption and depletion.[1] This theory incorporates the polymer-surface and polymer-solvent interaction and is applicable to any chain length (monomers, oligomers, long chains) and any polymer concentration (from very dilute solutions up to the polymer melt). Because the segments have a finite volume, it is easy to account for the volume-filling constraint. The interaction between polymer and solvent (including the volume-filling constraint) is described by extending the classical Flory-Huggins (FH) theory[9] for homogeneous polymer solutions to a concentration gradient: here the FH solvency parameter χ enters, which in most cases (segment-solvent repulsion) is positive. The interaction between polymer and surface is a square-well potential with depth (for attraction) or height (for repulsion) ε; the usual parameter is $\chi_s = \varepsilon/kT$, so that the temperature T is automatically included (unlike in the continuum model, see below). The value of χ_s is positive for repulsion and negative for attraction. Note that we use a different sign of χ_s as compared to the original definition by Silberberg,[10] copied ever since.[1] Our present convention is in line with the general custom

in physics that attraction is counted negative and repulsion positive.

The disadvantage of this SCF theory is that only numerical results are obtained, which makes it sometimes difficult to recognize the general trends. Another problem is that it cannot easily deal with swelling of excluded-volume chains in a good solvent (although recently extensions in this direction were described).[11,12]

Analytical theories use a continuum model for the polymer chain. Chain configurations are described as Brownian trajectories in a field and the end-point distribution satisfies the Edwards diffusion equation.[13] The interaction with the surface is not a square-well potential but a given extrapolation length $1/c$, for which the relation with T is unknown. For simple cases (in the limit of infinite dilution) an exact solution of the Edwards equation can be obtained. For finite concentrations an exact analytical solution is impossible but in many situations a ground-state approximation (GSA) enables simplifications which give insight in the trends.

Because the finite segment volume is neglected in the continuum theory, this model cannot account for the volume-filling constraint. This is not a serious problem for repulsive polymer-surface interactions (i.e., polymer depletion) since then the polymer concentrations are low everywhere. However, for attractive interactions (polymer adsorption) this leads to some unrealistic divergences, especially for strong adsorption.

In classical double-layer theory an analogous problem occurs. The continuum Poisson-Boltzmann (PB) theory,[14] where the finite ion size is neglected, predicts unrealistically high counterion concentrations close to a highly charged surface. This problem was solved long ago by Stern[15] who introduced what is now called the Stern layer, with a thickness corresponding to the size of a (hydrated) ion. Thus, the Stern layer incorporates the finite ion size into continuum PB theory.

We adopt a similar procedure for the continuum theory for polymers at interfaces. We insert the lattice boundary condition, which contains the adsorption energy χ_s and the volume-filling condition accounting for the finite segment size, into the continuum equations (exact for infinite dilution, GSA for finite concentrations). This serves a dual purpose. First, it introduces the finite segment volume into the continuum model, so that the divergence for strong adsorption is eliminated: the train volume fraction can never exceed unity. Second, it gives a general relation between the continuum parameter c and the lattice parameter χ_s, so that for any adsorption energy χ_s the c parameter is directly obtained and the analytical continuum equations can be used to interpret numerical SCF data and to predict experimental trends. In addition, the relation between c and T is now known.[16]

We apply this concept to both the depletion and adsorption regimes. For depletion the volume filling is not important and the relation between c and χ_s is very simple: $\Delta\chi_s = \ln(1 + c/5)$, with $\Delta\chi_s = \chi_s - \chi_{sc}$; here $\chi_{sc} = \ln(5/6) + \chi/6$ is the critical adsorption energy for long chains on a simple cubic lattice. Note that the sign of χ_{sc} is different from the original definition[10,17] because we use positive χ_s for repulsion. For $\chi = 0$ (very good solvent) the relation $c(\chi_s)$ is the same as derived before for a single ideal chain;[18] again the signs of c and $\Delta\chi_s$ are different. SCF computations for the end-point distribution using this relation give, in the dilute limit, quantitative agreement with the analytical solution of the Edwards equation. A good approximation for the concentration profile is $\rho = \tanh^2[(z + p)/\delta_d]$, where ρ is the segment density normalized on the bulk solution and δ_d is the depletion thickness in the dilute limit, which is close to the radius of gyration $R \sim N^{1/2}$. The shift p, which also may be denoted as *proximal* length (as opposed to the "distal" or decay length δ_d), equals the extrapolation length $1/c$ for strong repulsion; then p is nearly zero. For weaker repulsion p is no longer small; it is, however, a known function of c and δ_d.

For semidilute solutions the classical approximation for strong repulsion is $\rho = \tanh^2(z/\xi)$,[19] where the correlation length (= semidilute depletion thickness) ξ depends only on the concentration in the bulk solution (and on solvency) but not on chain length. We generalize this relation in two respects. First, we replace ξ by a depletion thickness δ defined by $\delta^{-2} = \delta_d^{-2} + \xi^{-2}$ (Refs. 20 and 21) which makes δ a function of both chain length and concentration; this relation reduces to the two limits ($\delta = \delta_d$ for dilute solutions and $\delta = \xi$ for the semidilute case) but is also valid for intermediate concentrations. Second, we apply a similar shift p as in dilute solutions, which covers also the case of weak repulsion. Hence, we use $\rho = \tanh^2[(z + p)/\delta]$, where again two length scales p (proximal) and δ (distal) occur. For strong repulsion $p = 1/c$ (then the proximal length equals the extrapolation length), for weak repulsion p depends also on δ (then p is smaller than the extrapolation length). For mean field, we find nearly quantitative agreement with numerical SCF profiles, for good and theta solvents and for dilute and semidilute solutions. This equation is also valid for excluded-volume chains in a good solvent; the only modification here is that we have to insert the correct scaling exponents (and numerical prefactors) for the depletion thickness δ, as proposed earlier.[21]

The adsorption case is more difficult to describe analytically,[22] because the local concentrations are much higher; moreover, tails contribute to the concentration profile. However, close to the surface tails may be neglected, and it is sufficient to consider only the ground-state function for trains and loops (and in semidilute solutions also for free chains). Inserting the lattice boundary condition into these ground-state functions, which are different for the dilute and semidilute regimes, gives, nevertheless, the *same* relation $\Delta\chi_s(c)$ for the adsorption branch in the two regimes. This relation is therefore valid for any concentration. In addition, we find a very simple equation for the train density φ_0 as a function of the adsorption energy. Again this equation applies to any concentration. Comparison with numerical SCF shows excellent agreement.

This paper is organized as follows. In Sec. II we summarize the basics of the SCF lattice model. In Sec. III we briefly describe the continuum model. We discuss the exact solution for a single chain next to a surface[23,24] and compare this with SCF results for the depletion regime, using $\Delta\chi_s = \ln(1 + c/5)$ for the conversion of c to $\Delta\chi_s$. We present some simplifications for depletion: a tanh profile for end-points and a $\tanh^2$ profile for the overall segment concentration. In

Sec. IV we describe the GSA formalism and the general relation $\Delta\chi_s(c)$, for both depletion and adsorption. In Sec. V we apply this formalism to depletion of non-ideal chains at finite concentrations and we compare again with numerical SCF results. In Sec. VI we do the same for adsorption, where we have to discriminate between good and theta solvents. In both cases (adsorption and depletion) the relation $\Delta\chi_s(c)$ is valid for the entire concentration regime and it is independent of chain length. We suggest some methods to determine c or $\Delta\chi_s$ from experiments.

Two appendices present some mathematical background. In Appendix A we give the full (complicated) Eisenriegler solution[25] for the concentration profile of an ideal chain and we discuss a simplified $\tanh^2$ approximation for this profile in the case of depletion. In Appendix B we describe several versions of the GSA-simplification of the Edwards equation: adsorption and depletion from semidilute solutions, and adsorption from dilute solutions, with one version for good solvents and another for a theta solvent in all cases.

II. LATTICE MODEL

A. Field

We restrict ourselves in this paper to a simple six-choice cubic lattice and to two solution components: a homopolymer in a monomeric solvent next to a solid surface. In the Scheutjens-Fleer model the walks representing the polymer chain take place in a (dimensionless) field u_z given by[1,22]

$$u_z = u_z^a - 2\chi[\langle\varphi_z\rangle - \varphi^b] - \ln\frac{1-\varphi_z}{1-\varphi^b}$$
$$u_z^a = \begin{cases} \chi_s - \chi/6 & z = 0 \\ 0 & z > 0 \end{cases}, \tag{1}$$

where z is the layer number, with $z = 0$ for the train layer next to the surface. The reference point is the bulk solution, where $u = 0$. The adsorption energy term u_z^a is a step function and is only non-zero for train segments ($z = 0$); χ_s is the adsorption energy of a polymer segment (with respect to solvent) and χ is the FH solvency parameter.[9] The term $\chi/6$ accounts for the one missing contact with solvent for a train segment. Unlike in the original literature[1,10,22] we define χ_s to be positive for repulsion and negative for attraction.

The second term in Eq. (1) is the solvency contribution, which depends on χ and the polymer volume fractions φ_z in layers z and φ^b in the bulk solution; it is the extension of the classical FH expression[9] towards a concentration gradient. The angular brackets represent the non-local effect in the gradient:

$$\langle\varphi_z\rangle = \frac{1}{6}\varphi_{z-1} + \frac{4}{6}\varphi_z + \frac{1}{6}\varphi_{z+1}. \tag{2}$$

The logarithmic term in Eq. (1) accounts for the volume filling, as in FH; it ensures that φ_z can never exceed unity.

Equation (1) allows to compute the field $\{u\}$ from the concentration profile $\{\varphi\}$; the braces indicate a set of M values ($z = 0, 1 \ldots M-1$), with layer M somewhere in the bulk solution.

B. Propagator

We define the end-point distribution $G_{z,s}$ that a walk of s segments ($s-1$ steps) in a given field $\{u\}$ ends in layer z. For a monomer we abbreviate $G_{z,1}$ as G_z, which is simply the Boltzmann weight of the field:

$$G_z = G_{z,1} = e^{-u_z}. \tag{3}$$

Thus, $G_\infty = 1$. For a dimer we have $G_{z,2} = G_z(G_{z-1,1} + 4G_{z,1} + G_{z+1,1})/6$ and we see a similar neighbor average as in Eq. (2). For a segment s we relate the weight to that of the previous segment $s-1$:

$$G_{z,s} = G_z\langle G_{z,s-1}\rangle, \tag{4}$$

where

$$\langle G_{z,s}\rangle = \frac{1}{6}G_{z-1,s} + \frac{4}{6}G_{z,s} + \frac{1}{6}G_{z+1,s}. \tag{5}$$

From Eqs. (3) and (4) we can compute from a given field the distribution $G_{z,N}$ and the volume fraction φ_z^e of the end-point of a chain of N segments:

$$\varphi_z^e = CG_{z,N} \qquad C = \varphi^b/N \tag{6}$$

The normalization factor C is given by the fact that in the bulk solution (where $G_{z,N} = 1$) φ^e equals $1/N$ times the overall concentration φ^b.

C. Composition law

The concentration $\varphi_{z,s}$ of some interior segment s in a chain 1.. s.. N is found from combining two walks from either end-point:

$$\varphi_{z,s} = Ce^{u_z}G_{z,s}G_{z,N-s+1}. \tag{7}$$

The factor $e^{u_z} = 1/G_z$ corrects for double counting segment s (which is included in both walks); it accounts for the finite segment size. In the continuum model Eq. (7) is used in the form $\varphi(z, s) = CG(z, s)G(z, N-s)$; then the factor e^{u_z} is omitted. For $s = 1$ or N Eq. (7) reduces to Eq. (6). The overall polymer profile is

$$\varphi_z = \sum_{s=1}^{N}\varphi_{z,s}. \tag{8}$$

Equation (8) gives the concentration profile $\{\varphi\}$ as a function of $\{u\}$. The field $u(\varphi)$ (Eq. (1)) should be consistent with the profile $\varphi(u)$ (Eq. (8)). These two relations thus constitute a set of M equations in M variables $\varphi_0, \varphi_1 \ldots \varphi_{M-1}$ (or $u_0, u_1 \ldots u_{M-1}$), which set can be solved by numerical iteration. Then the concentration profile $\varphi_{z,s}$ is known for any ranking number s in the chain.

III. CONTINUUM MODEL

A. Edwards equation

In a continuum model non-integer values of z and s are allowed, so we change notation from $G_{z,s}$ to $G(z,s)$. Edwards[13] derived the following differential equation for the end-point

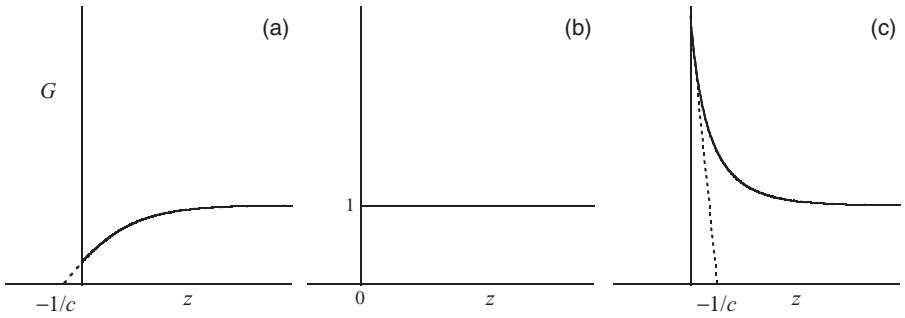

FIG. 1. Illustration of the extrapolation length $1/c$. The initial tangent of $G(z, s)$ extrapolated to the z axis hits this axis at $z = -1/c$. For depletion (a) the intercept is negative and c is positive, for adsorption (c) the intercept is positive and c is negative. At the critical point (b) $G = 1$ for any z, so $1/c = \infty$ and $c = 0$.

distribution $G = G(z, s)$ in a field $u = u(z)$:

$$\partial^2 G/\partial z^2 = 6\,(\partial G/\partial s + uG)\,. \tag{9}$$

It has been shown[1,26] that Eq. (9) is the continuum version of the discrete lattice propagator (Eq. (4)).

The definition of $z = 0$ requires special attention. The space $z > 0$ is accessible to (the center of) a segment, so it is sensible to put $z = 0$ not at the surface but half a bond length away from it. This is analogous to defining $z = 0$ for the (middle of the) train layer in the lattice model.

The boundary condition for solving Eq. (9) is[19,23,24]

$$G^{-1}\partial G/\partial z|_{z=0} = c, \tag{10}$$

where c is the inverse extrapolation length. Its physical meaning is illustrated in Fig. 1.

At the critical point G does not depend on z so $c = 0$. In the adsorption regime G decreases with z and c is negative, for depletion c is positive. The parameter c measures the interaction with the surface so it should be related to χ_s as used in the lattice model. The precise relation is discussed later. Anticipating this discussion we mention already that for depletion at $\chi = 0$ we have $c = 6e^{\chi_s} - 5$ or $\chi_s = \ln[(5 + c)/6]$ (Eq. (22)); at the critical point $\chi_s = \chi_{sc} = \ln(5/6)$. In Sec. III B we use this relation to compare the continuum solution of the Edwards equation with numerical SCF data.

B. Exact solution of the Edwards equation

Exact solutions of Eq. (9) are only known for zero field ($u = 0$). Lepine and Caillé[23] and later Eisenriegler *et al.*[24] derived the now classical equation for the Green function $G = G(z,N)$ of a freely floating ideal chain next to an adsorbing or repelling surface, with an interaction parameter c as defined in Eq. (10):

$$G = \mathrm{erf}\,\zeta + e^{-\zeta^2}\,Y(\zeta + C), \tag{11}$$

where the scaled z-coordinate ζ and the scaled c-parameter C are defined in terms of the radius of gyration R. These parameters and the function $Y(x)$ are given by

$$R = \sqrt{N/6} \quad \zeta = z/2R \quad C = cR \quad Y(x) = e^{x^2}\mathrm{erfc}x. \tag{12}$$

The function $Y(x)$ decreases monotonically with increasing x: it equals $2e^{x^2}$ for large negative x, is unity at $x = 0$, and decays as $1/(x\sqrt{\pi})$ for large positive x.

For $z = 0$, $G_0 = G(0,N)$ equals $Y(C)$, which is below unity for positive c (with $G_0 = 1/(C\sqrt{\pi})$ for strong repulsion), equals 1 at the critical point $c = 0$, and becomes very large for $c < 0$ (with $G_0 = 2e^{C^2}$ for strong attraction). The initial slope $(\mathrm{d}G/\mathrm{d}z)_0$ is cG_0 or $(\mathrm{d}G/\mathrm{d}\zeta)_0 = 2CG_0$ (Eq. (10)). We note that $G_0 = Y(C)$ is the partition function of an end-grafted chain.

The region $C > 1$ is the regime of strong repulsion (strong depletion) and the region $C < -1$ the regime of strong adsorption. The region $-1 < C < 1$ around the critical point is the regime of weak adsorption or weak depletion.

Figure 2(a) (solid curves) shows the Green function G as a function of $\zeta = z/2R$ for four positive values of $C = cR$, representative for very weak ($C = 1/\sqrt{60}$, $c = 0.01$ for $N = 1000$) to strong repulsion ($C = 100/\sqrt{60}$, $c = 1$ for $N = 1000$). All curves start at a level $Y(C)$ for $\zeta = 0$, have an initial slope $2CY(C)$, and reach the limit 1 for large ζ.

The symbols in Fig. 2(a) are numerical SCF results for $\chi = 0$ and a very low volume fraction (10^{-7}) in the bulk solution, for various chain lengths: $N = 10, 40, 100, 4000$. At this low concentration the mutual interactions between the polymer segments are negligible: the second and third terms in Eq. (1) vanish and the field is a simple step function $u_0 = \chi_s$ and $u_z = 0$ for $z > 0$. The SCF results (at fixed φ^b and χ) require N and χ_s as input, so we obtain the end-point distribution $G(z, N, \chi_s)$ with three parameters. Using $\chi_s = \ln[(5 + c)/6] = \ln[(5 + C/R)/6]$ we can obtain $G(\zeta,C)$ with only two parameters. Note, however, that for fixed C we now have to choose a different χ_s (or c) for any N: the c values in Fig. 2 are $c\sqrt{10N} = 1,\ 4,\ 10,\ 100$.

From Fig. 2(a) it is clear that for long chains there is quantitative agreement between the continuum and lattice models. For strong repulsion also the results for short chains coincide with the continuum model, down to $N = 10$. For weaker repulsion there is a minor but systematic deviation, which becomes more pronounced the shorter the chains are. It is gratifying to note that the SCF results for various N (above $N = 100$) collapse onto a universal curve for given C, even for weak repulsion.

Therefore the Green function $G(z, N, c)$ (Eq. (11)) for a continuum chain may be converted to the Green function

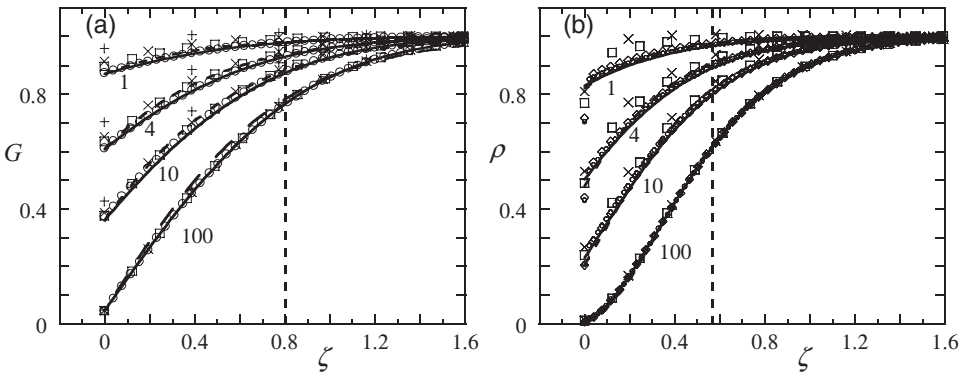

FIG. 2. The end-point distribution G of an ideal chain (a) and its density profile ρ (b) as a function of $\zeta = z/2R$, for four positive values of $C = cR$: $C\sqrt{60} = 1, 4, 10, 100$. Solid curves are the exact Eq. (11) (a) or Eq. (A1) (b). Dashed curves are the approximation according to Eq. (13) (a) or Eq. (14) (b). Symbols are numerical SCF data for a 6-choice lattice, $\chi = 0$, and $\varphi^b = 10^{-7}$, for different chain lengths: $N = 4000$ (circles), 100 (squares), 40 (crosses), 10 (plusses) in (a), and 4000 (circles), 1000 (diamonds), 100 (squares), 40 (crosses) in (b). The c values were converted to the lattice parameter χ_s as discussed in the text. The vertical dashed line in (a) is $\zeta = \delta_e/2R = \sqrt{2/\pi}$, that in (b) $\zeta = \delta_d/2R = \sqrt{1/\pi}$.

$G(z, N, \chi_s)$ for a lattice chain, using a simple relation $c(\chi_s)$. This conversion is accurate for strong and weak repulsion and for any chain length, down to oligomers ($N \approx 10$). It was established before[18,32] that the partition function of an end-grafted ideal lattice chain in the depletion regime can be written as $G(0, N, c) = Y(cR)$ and the same relation between c and χ_s. Recently,[16] it was shown that mechanical desorption of a lattice chain by an external force can also be expressed by analytical equations derived from a continuum model and a simple relation $c(\chi_s)$ for the adsorption branch.

From Eq. (11) the density profile ρ (normalized on $\zeta = \infty$) of monomers of an ideal chain may be computed using the continuum version of the composition law (Eq. (7)). The result as derived by Eisenriegler[25] is given in Eq. (A1) of Appendix A. The solid curves in Fig. 2(b) show the exact $\rho(\zeta, C)$ for the same four C values as in Fig. 2(a). Again the symbols are numerical SCF results, for $N = 40$, 100, 1000, 4000. For strong repulsion the agreement is of the same level as in Fig. 2(a), for weaker repulsion it is quite good for all layers $z \geq 1$ but there is a systematic deviation for $z = 0$. This deviation is due to a subtle difference in the composition law used in the two models. In the continuum theory the factor e^{μ_z} in Eq. (7) is set unity. In SCF this factor (for low φ^b) is essentially unity for all $z > 0$ because $u \approx 0$; that is why the two models agree quite well for $z > 0$. However, for $z = 0$ it is $e^{\chi_s} = (5 + c)/6$. Hence, close to the critical point (very small c) $\rho_0 \approx 5/6$ in SCF, whereas Eq. (A1) gives $\rho_0 = 1$ for $c \to 0$.

Anyhow, the SCF results for long enough chains collapse again onto a universal curve for given C. For short chains the deviations at weak repulsion are bigger for ρ (Fig. 2(b)) then for G (Fig. 2(a)).

C. Approximations for depletion

It is well known that for depletion the ground-state end-point distribution is approximately a tanh function (see Sec. V A). Also Eq. (11) for positive C can be approximated by such a function. Then we use $g_e = \tanh[a\zeta + b]$ as an approximation to G; the subscript $_e$ refers to the end-point distribution. The constant a determines the width of the distribution, the shift b is fixed by the initial value $g_e(\zeta = 0) = G_0$, or $b = \operatorname{atanh} G_0$. It turns out that $a = \sqrt{\pi/2}$ works well (see Eq. (A8) in Appendix A). Hence,

$$g_e = \tanh\left(\sqrt{\frac{\pi}{2}}\zeta + \operatorname{atanh} Y(C)\right), \tag{13}$$

where again only the two parameters ζ and C occur. The dashed curves in Fig. 2(a) show that Eq. (13) is a good approximation to the exact G. For strong repulsion the shift b is small and $g_e = \tanh(z/\delta_e)$, where $\delta_e = \sqrt{8/\pi}R$ is the depletion thickness for end points.

In the ground-state spirit the overall density profile is approximately a $\tanh^2$ function (see also Sec. V A). So we try $\rho = \tanh^2[a\zeta + b]$ where a determines the width of the overall distribution and b is fixed by $\rho(\zeta = 0) = \rho_0$. Now $a = \sqrt{\pi}$ is appropriate:[20] the "average" segment is closer to the surface than the end-point. A good approximation for ρ_0 is $\rho_0 = Y^2(C/\sqrt{2})$ (Eq. (A7)). Hence, Eq. (A1) may be approximated as

$$\rho = g^2 \quad g = \tanh\left(\sqrt{\pi}\zeta + \operatorname{atanh} Y\left(\frac{C}{\sqrt{2}}\right)\right). \tag{14}$$

The dashed curves in Fig. 2(b) demonstrate that Eq. (14) works quite well. For strong repulsion $\rho = \tanh^2(z/\delta_d)$, where $\delta_d = (2/\sqrt{\pi})R$ is the depletion thickness for overall segments. The subscript $_d$ means "dilute" (later, Eq. (26), we shall use the symbol δ for a generalized depletion thickness). The depletion thickness $\delta_d = 1.13R$ for "average segments" is smaller than $\delta_e = 1.60R$ for end segments by a factor of $\sqrt{2}$.

In Sec. V (Fig. 5) we show that a $\tanh^2$ function for ρ is also a good approximation for depletion of non-ideal chains at finite concentrations. However, we then have to use a different definition of the depletion thickness δ, which becomes a function of concentration.

IV. GROUND-STATE APPROXIMATION AND THE RELATION $c(\chi_s)$

A. GS equation

In Sec. III B we considered ideal chains in zero field (very dilute solutions), where an exact solution of the

Edwards equation is available. For finite concentrations the field is nonzero and one can find only approximate solutions. The standard procedure is to expand $G(z, s)$ as an infinite sum over $g_k(z)e^{\varepsilon_k s}$, where g_k is the kth eigenfunction and ε_k the corresponding eigenvalue. This expansion is exact but does not yet help in finding analytical solutions. In the GSA only the leading term in the expansion, corresponding to the ground state (GS), is retained. Hence, the function $G(z, s)$ is approximated as

$$G(z, s) = g(z)e^{\varepsilon s}, \tag{15}$$

where g is the GS function and ε the GS eigenvalue. The z and s dependencies are now separated. In GSA the effect of the ranking number is neglected, in the sense that all segments are assumed to have the same spatial distribution: all segments, even those close to the chain ends, are approximated as "middle" segments.

With Eq. (15) the Edwards equation (Eq. (9)) reduces to the simpler GS equation,

$$d^2g/dz^2 = 6(\varepsilon + u)g, \tag{16}$$

which is an ordinary second-order differential equation in one variable z.

In order to solve Eq. (16) we need the value of ε and an expression for the field u. We first consider those situations where g reaches a constant non-zero value in the bulk solution. This is the case when g refers to the overall profile, as in depletion and in adsorption from semidilute solutions. In those situations $\varepsilon = 0$ because both d^2g/dz^2 and u vanish for large z. Later (Sec. VI B) we shall also discuss adsorption from dilute solutions, where g describes only the loop profile. Then $g = 0$ in the bulk solution and $\varepsilon \neq 0$.

The field u is given by Eq. (1) without the term u^a: in the continuum model the interaction with the surface is expressed through the continuum boundary condition (the extrapolation length). However, the nonlocal term $\langle\varphi\rangle$ and the logarithmic volume-filling term frustrate an analytical solution of Eq. (16). When we neglect the non-local effect by assuming $\langle\varphi\rangle = \varphi$ and expand the term $\ln(1-\varphi)$ to lowest order we obtain

$$u = \begin{cases} v(\varphi - \varphi^b) & \textit{good solvent} \\ [\varphi^2 - (\varphi^b)^2]/2 & \textit{theta solvent} \end{cases} \qquad v = 1 - 2\chi, \tag{17}$$

where v is the Edwards excluded-volume parameter.

The volume fraction $\varphi = \varphi(z)$ is proportional to g^2 as follows from the composition law (Eq. (7)). Substituting Eq. (15) with $\varepsilon = 0$ into Eq. (7) (and omitting e^{u_z}) leads to $\varphi(z, s) = N^{-1}\varphi^b g^2$, which demonstrates that in GSA the distribution does not depend on the ranking number s. Hence, $\varphi = \varphi^b g^2$, which gives $g = 1$ in the bulk solution, as expected from Eq. (15) with $\varepsilon = 0$. Equation (17) for semidilute solutions transforms into

$$u = \begin{cases} v\varphi^b(g^2 - 1) & \textit{good} \\ (\varphi^b)^2(g^4 - 1)/2 & \textit{theta} \end{cases}. \tag{18}$$

For adsorption from dilute solutions ($\varepsilon \neq 0$) we have $\varphi = g^2$ (see Sec. VI B); then a good approximation is $u = vg^2$ for a good solvent and $u = g^4/2$ for a theta solvent (Eq. (B7)).

Inserting $u(g)$ into Eq. (16) gives a differential equation d^2g/dz^2 as a function of g, which may be solved to give an explicit form $g(z)$. This form depends on conditions (good or theta solvent, depletion or adsorption, dilute or semidilute solutions). Some mathematical details are presented in Appendix B, and the solution $g(z)$ is given in Sec. V A for depletion, and in Secs. VI A and VI B for adsorption.

B. The GSA boundary condition

The continuum boundary condition (Eq. (10)) expresses the initial slope $\partial G/\partial z|_0$ as cG_0, where $G_0 = G(0, s)$ is the value of the Green function at $z = 0$ and c is the inverse extrapolation length (see Fig. 1). In GSA (Eq. (15)) this translates to $dg/dz|_0 = cg_0$, with $g_0 = g(0)$. The crucial point in this paper is that we account for the finite segment size: we replace the continuum derivative $dg/dz|_0$ by the discrete form $g_1 - g_0$, with $g_1 = g(1)$. Again this is analogous to double-layer theory, where the electrical potential is linear across the Stern layer. Hence, we use the following boundary condition:

$$c = g_1/g_0 - 1. \tag{19}$$

At the critical point $c = 0$ because $g_1 = g_0$. For depletion $g_1/g_0 > 1$, so c is positive. For adsorption $g_1/g_0 < 1$ and c is negative; since the minimum value of g_1 is zero, c has to be above -1. Thus, for strong adsorption c reaches a minimum value of order -1 with our discrete boundary condition, which, as we shall see, limits the train volume fraction φ_0. With the original continuum version $c = g^{-1}dg/dz$, c could decrease without bounds, leading to the unrealistic behavior that φ_0 would exceed unity.

In Sec. V A we shall see that for depletion g is indeed linear in z for small z; in that case there is no difference between the continuum and discrete variants of the boundary condition. For adsorption, where $g \sim (z + p)^{-1}$ for good solvents and $g \sim (z + p)^{-1/2}$ for theta solvents (see Sec. VI), there is a difference. We prefer the discrete variant since the train layer ("Stern layer") is discretized and φ_0 has a natural limit $\varphi_0 = 1$.

C. The lattice boundary condition

The lattice boundary condition does not use the c parameter but involves the field u_0 for segments at $z = 0$, which contains the adsorption energy χ_s and the volume-filling constraint. This boundary condition is simply the propagator (Eq. (4)) for train segments ($z = 0$), where one term ($z = -1$) is absent. For $z = 0$ and $s = N + 1$ Eq. (4) reads $G_{0,N+1} = G_0(4G_{0,N} + G_{1,N})/6$ or $6e^{u_0} = (4G_{0,N} + G_{1,N})/G_{0,N+1}$. We translate this to the continuum model as

$$6e^{u_0} = \frac{4G(0, N) + G(1, N)}{G(0, N + 1)} = 4 + \frac{g_1}{g_0}, \tag{20a}$$

$$6e^{u_0} = 5 + c. \tag{20b}$$

The second form of Eq. (20a) is GSA according to Eq. (15), whereby we neglected the difference between N and $N+1$ when $\varepsilon \neq 0$ (adsorption from dilute solutions). Equation (20b) was obtained by inserting the GSA boundary condition (Eq. (19)) into Eq. (20a). It demonstrates that by combining the boundary conditions in the two models a direct relation between the extrapolation length and the field u_0 is found. This relation is the basis of our attempt to reconcile the analytical continuum theory with the numerical SCF model.

D. The relation $c(\chi_s)$

According to Eq. (20b) $c = 6e^{u_0} - 5$, where u_0 is given by Eq. (1). For depletion the volume filling plays no role and the concentration terms in Eq. (1) are small; then the simple form $u_0 = \chi_s - \chi/6$ is sufficient. Hence, $c = 6e^{\chi_s - \chi/6} - 5$ for depletion; this is the form used in Fig. 2 (for $\chi = 0$) to compare the exact continuum solutions with SCF.

It is convenient to use a difference parameter $\Delta\chi_s$ which measures the deviation from the critical point and which is positive for depletion and negative for adsorption. In a six-choice cubic lattice the critical point separating the adsorption and depletion regimes for long chains at $\chi = 0$ is situated at $\chi_{sc} = \ln(5/6)$; this is the same form as in Ref. 17 apart from the sign. For $\chi > 0$ the critical adsorption energy is less negative by an amount $\chi/6$ because of the one missing segment-solvent contact for an adsorbed segment; then $\chi_{sc} = \ln(5/6) + \chi/6$. Hence, we define

$$\Delta\chi_s = \chi_s - \chi_{sc} \quad 6e^{\chi_s - \chi/6} = 5e^{\Delta\chi_s}. \tag{21}$$

At the critical point $\Delta\chi_s$ is zero, like the c parameter in the continuum model.

We obtain now a very simple relation between c and χ_s for depletion:

$$c = 5(e^{\Delta\chi_s} - 1) \quad c = 5\Delta\chi_s \quad around\ cp. \tag{22}$$

This equation (for $\chi = 0$) was first derived for a single ideal end-grafted chain, using the full expression in Eq. (20a) and $G(z, N)$ obtained from an exact solution of the Edwards equation (with $u = 0$) for the end-grafted case.[18,32] Equation (22) turns out to be *generally* valid, also for non-ideal chains with $\chi \neq 0$ and for any concentration and chain length.

In Fig. 3 we plot $c(\Delta\chi_s)$ according to Eq. (22) (solid curve, with the limit $c = 5\Delta\chi_s$ shown as the dotted line), and we compare with numerical SCF results for $N = 1000$, $\varphi^b = 10^{-6}$, and five solvencies. These SCF data were obtained from Eq. (19) in the form $c = G_1/G_0 - 1$, with for the G's the numerical end-point concentrations. The agreement between the numerical data and Eq. (22) is excellent. There is no dependence on solvency. Also, there is essentially no effect of the chain length or the bulk solution concentration: in the numerical SCF data there is hardly any difference in G_1/G_0 between $N = 100$ and $N = 1000$, or between $\varphi^b = 10^{-6}$ (dilute) and $\varphi^b = 10^{-2}$ (semidilute).

For adsorption we cannot neglect the concentration terms in the field because the volume filling is important (and even dominates for strong adsorption): $u_0 = \chi_s - \chi/6 - 2\chi\langle\varphi_0\rangle - \ln(1-\varphi_0)$, where in Eq. (1) we neglected φ^b with respect to φ_0. Hence, $6e^{u_0} = 5e^{\Delta\chi_s}e^{-2\chi\langle\varphi_0\rangle}/(1-\varphi_0)$. According to Eq. (2) $\langle\varphi_0\rangle = (4\varphi_0 + \varphi_1)/6 = \varphi_0(4 + g_1^2/g_0^2)/6 = \varphi_0[4 + (1+c)^2]/6$. The general relation $c(\chi_s)$ is

$$5e^{\Delta\chi_s} = (5+c)(1-\varphi_0)\exp\left(\chi\varphi_0\frac{4+(1+c)^2}{3}\right). \tag{23}$$

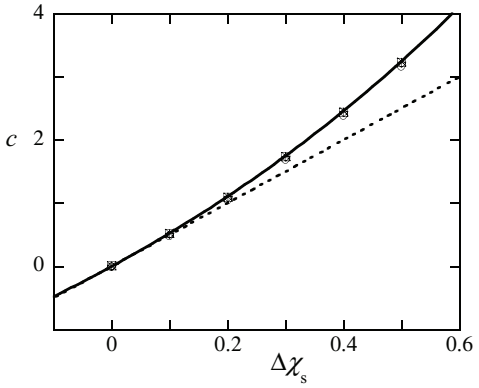

FIG. 3. Theoretical and numerical results for the inverse extrapolation length c as a function of $\Delta\chi_s$ for depletion. The solid curve is Eq. (22), the dotted line is $c = 5\Delta\chi_s$. Symbols are numerical SCF data for five solvencies: $\chi = 0$ (circles), 0.3 (diamonds), 0.4 (squares), 0.45 (plusses), and 0.5 (crosses).

For depletion φ_0 is small and Eq. (23) reduces to Eq. (22). For adsorption (Sec. VI) φ_0 may be high; we then need the relation between φ_0 and c, which is different for good and theta solvents. We discuss this relation later (Eq. (33)).

V. DEPLETION RESULTS

A. Explicit expressions for $g(z)$

We start with the ideal-chain result of Eq. (14): $\rho = g^2$ with $g = \tanh[(\sqrt{\pi}/2R)z + \operatorname{atanh}Y(cR/\sqrt{2})] = \tanh[(z+p)/\delta_d]$, where $\delta_d = 2R/\sqrt{\pi}$ is the depletion thickness in the dilute limit and the proximal length p is given by $p = \delta_d \operatorname{atanh}Y\left(c\delta_d\sqrt{\pi/8}\right)$. For strong repulsion (large c), where $Y(x) = 1/(x\sqrt{\pi})$, this gives $p = (\sqrt{8}/\pi)/c = 0.9/c$. This result is not quite correct, as follows from $g_1/g_0 = 1 + c$ (Eq. (19)). For strong repulsion $g_0 = p/\delta_d$ and $g_1 = (1+p)/\delta_d$ are small and the ratio g_1/g_0 equals $1 + 1/p$. Hence, $p = 1/c$ in this limit. We therefore change $\sqrt{\pi/8}$ in the above expression for p to $1/\sqrt{\pi}$:

$$g = \tanh\frac{z+p}{\delta_d}, \tag{24a}$$

$$\delta_d = \frac{2R}{\sqrt{\pi}}, \tag{24b}$$

$$p = \delta_d \operatorname{atanh} Y\left(\frac{c\delta_d}{\sqrt{\pi}}\right). \tag{24c}$$

Equation (24c) relates p to c for both weak and strong repulsion. For weak repulsion p depends also on δ_d. A plot $p(1/c)$ according to Eq. (24c) is given in Fig. 4 (top curve).

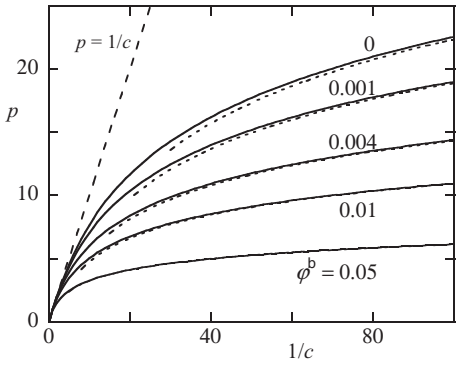

FIG. 4. The proximal length p as a function of the extrapolation length $1/c$ for depletion, for $\chi = 0$ and $N = 1000$. Solid curves are Eq. (26c) for $\varphi^b = 0$, 0.001, 0.004, 0.01, and 0.05. The dashed line is the strong repulsion limit $p = 1/c$ (Eq. (27a)). The dotted curves are the logarithmic form (Eq. (27b)) for weak repulsion.

Equation (24) applies to dilute solutions. For semidilute solutions we use GSA. Substituting $\varepsilon = 0$ and $u(g)$ from Eq. (18) into Eq. (16) gives two simple differential equations (Eq. (B2)), one for good solvents and one for a theta solvent. As shown in Appendix B the solution is

$$g = \tanh \frac{z + p}{\xi}, \tag{25a}$$

$$\xi = \begin{cases} 1/\sqrt{3v\varphi^b} & good \\ 0.658/\varphi^b & theta \end{cases}, \tag{25b}$$

$$p = \xi \operatorname{atanh} Y\left(\frac{c\xi}{\sqrt{\pi}}\right). \tag{25c}$$

The numerical factor for a theta solvent is $\operatorname{atanh}(1/\sqrt{3}) = 0.658$.

Equation (25) is valid for semidilute solutions, where the depletion thickness is the correlation length ξ, which depends only on the concentration: $\xi \sim \varphi^{-1/2}$ in good solvents and $\xi \sim \varphi^{-1}$ in a theta solvent. These are typical mean-field results. For a theta solvent this is adequate, but for excluded-volume chains in a good solvent the scaling exponent is different. We return to this point in Sec. V C.

The proximal length p in Eq. (25a) enters as an integration constant: when $g(z)$ is a solution of Eq. (B2), $g(z + p)$ is a solution as well. The expression for p given in Eq. (25c) is found by analogy with Eq. (24c): since Eq. (25a) can be found from Eq. (24a) by replacing the "dilute" depletion thickness δ_d by its semidilute analogue ξ, it is reasonable to apply the same substitution in Eq. (25c).

Again in Eq. (25c) $p = 1/c$ for strong repulsion, where p is small. This is the situation described by De Gennes[19] in his classical derivation of Eq. (25a). De Gennes discussed only good solvents and simply put $p = 0$. We consider also weak repulsion where p is nonzero; moreover, we also include a theta solvent. For weak repulsion p becomes also a function of φ^b.

Equations (24) and (25) describe two limiting cases. In dilute solutions the depletion thickness depends only on chain length (Eq. (24b)), in semidilute solutions it is only a function of concentration and solvency (Eq. (25b)). In previous papers[20,21] we proposed a generalized depletion thickness δ which reduces to the two limits δ_d (dilute) and $\xi = \delta_{sd}$ (semidilute) but applies to intermediate concentrations as well:

$$g = \tanh \frac{z + p}{\delta}, \tag{26a}$$

$$\frac{1}{\delta^2} = \frac{1}{\delta_d^2} + \frac{1}{\xi^2}, \tag{26b}$$

$$p = \delta \operatorname{atanh} Y\left(\frac{c\delta}{\sqrt{\pi}}\right), \tag{26c}$$

where δ_d is given by Eq. (24b) and ξ by Eq. (25b). Like Eq. (25c) was obtained from Eq. (24c) by substituting ξ for δ_d, Eq. (26c) is found by substituting the generalized δ.

We note that there is an alternative way to find an expression for $p(c,\delta)$. According to Eq. (19) we have $c = g_1/g_0 - 1 = \tanh[(1 + p)/\delta]/\tanh(p/\delta) - 1$. For strong repulsion ($\tanh x = x$) this gives $p = 1/c$, as expected. For weaker repulsion $\tanh(a + b) = (\tanh a + \tanh b)/(1 + \tanh a \tanh b)$ leads to a quadratic equation in the variable $\tanh(p/\delta)$, resulting in an explicit but clumsy analytical solution $p(c,\delta)$. The results are nearly identical to Eq. (26c), so we prefer this simple form.

It is useful to consider the limits of Eq. (26c):

$$p \approx 1/c \qquad 1/c < \delta/3, \tag{27a}$$

$$p \approx \frac{\delta}{2} \ln\left(\frac{\pi}{c\delta}\right) \qquad 1/c > 3\delta. \tag{27b}$$

These limits were obtained from $\tanh x = x$ for small x and $Y(y) = y^{-1}/\sqrt{\pi}$ for large y (Eq. (27a)), and $\tanh x = 1 - 2e^{-2x}$ for large x and $Y(y) = 1 - 2y/\sqrt{\pi}$ for small y (Eq. (27b)).

Figure 4 (solid curves) shows the proximal length p as a function of the extrapolation length $1/c$ according to Eq. (26c), for $N = 1000$, $\chi = 0$, and five concentrations. The dashed line is the strong-repulsion limit $p = 1/c$ (Eq. (27a)), valid for $1/c < \delta/3$ where δ varies from 14.6 at $\varphi^b = 0$ to 2.5 at $\varphi^b = 0.05$. The dotted curves give the logarithmic form of Eq. (27b) for weak repulsion, with a validity range $1/c > 3\delta$ (hence, $1/c > 45$ for $\varphi^b = 0$ and $1/c > 7$ for $\varphi^b = 0.05$). In dilute solutions $\delta = \delta_d$ so in the weak-repulsion limit p depends on c and N. On the other hand, in semidilute solutions p does not depend on N but only on c, φ^b, and χ. For intermediate concentrations p is a function of the four variables c, N, φ^b, and χ.

In Sec. V B (Fig. 5) we check the generalized Eq. (26) against SCF; we shall find that this generalization works quite well for both strong and weak repulsion.

B. GSA and SCF depletion profiles

Figure 5 gives the comparison between analytical GSA and numerical SCF depletion profiles for $\chi = 0$, $N = 1000$,

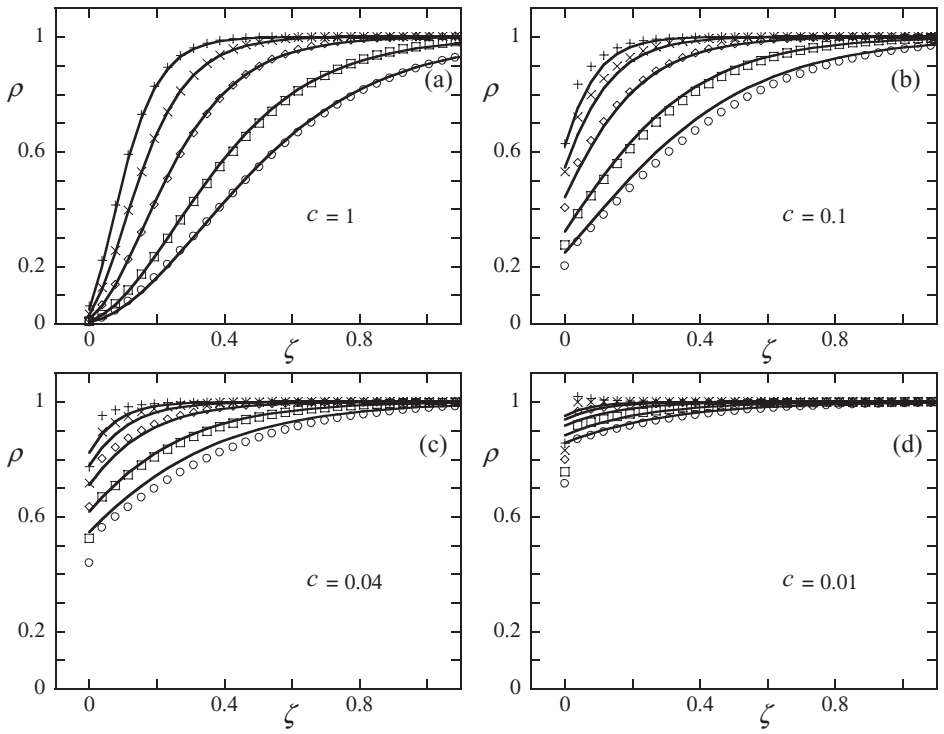

FIG. 5. Numerical (symbols) and analytical (curves) depletion profiles $\rho(\zeta)$ for $\chi = 0$, $N = 1000$, and five concentrations: $\varphi^{\mathrm{b}} = 10^{-7}$ (circles), 0.001 (squares), 0.004 (diamonds), 0.01 (crosses), and 0.02 (plusses). The interaction strength is $c = 1$, $C = 100/\sqrt{60}$ (a); $c = 0.1$, $C = 10/\sqrt{60}$ (b); $c = 0.04$, $C = 4/\sqrt{60}$ (c); and $c = 0.01$, $C = 1/\sqrt{60}$ (d). These are the same C values as in Fig. 2: the circles in each diagram (10^{-7}) are thus the same as in Fig. 2(b). The SCF results are for χ_{s} values computed from Eq. (22). The analytical curves are $\rho = g^2$ with g from Eq. (26).

five concentrations, and four values of c (the same as in Fig. 2). The χ_{s} values for the SCF data were obtained from Eq. (22). The analytical curves are Eq. (26): $\rho = g^2$ with g from Eq. (26a), δ from Eq. (26b), and p from Eq. (26c). The symbols for $\varphi^{\mathrm{b}} = 10^{-7}$ are the same as in Fig. 2(b), and the curves for this concentration are nearly the same (there is a minor difference in the definition of the shift p, as discussed above Eq. (24)).

For strong repulsion (Fig. 5(a)) the agreement is nearly quantitative: in this case p and $\rho_0 = \rho(0)$ are small and the main effect of an increasing concentration is to compress the depletion layer, as expressed by the depletion thickness δ in Eq. (26b). For weaker repulsion not only δ decreases with concentration, but ρ_0 increases because p is no longer small. The agreement between numerics and analytics is of the same level as in Fig. 2(b).

As discussed in connection with Fig. 2(b), the SCF data for $z = 0$ and weak repulsion are systematically lower than the continuum results, due to the factor e^{u_z} in the composition law (Eq. (7)). For $\chi = 0$ the factor e^{u_0} equals $e^{\chi_{\mathrm{s}}}(1 - \varphi^{\mathrm{b}})/(1 - \varphi_0) \approx e^{\chi_{\mathrm{s}}} = (5 + c)/6$. Hence, ρ_0 in SCF is roughly 5/6 of the GSA value when c is small. For $z > 0$ we have $u_z \approx 0$ and $e^{u_z} \approx 1$; then GSA and SCF are very close. For very weak repulsion and high φ^{b} (crosses in Fig. 5(d)) SCF gives $\rho_0 \approx 5/6$, as expected, whereas ρ_z for $z > 0$ is slightly above unity. Clearly, the GSA treatment cannot predict $\rho_z > 1$.

We may conclude from Fig. 5 that our analytical model describes the depletion data quite well. This does not only apply to $N = 1000$ and $\chi = 0$, but also to other chain lengths and solvencies.[20]

C. Extension to swollen chains

Figure 5 is for mean field and is based upon $\delta^{-2} = \delta_{\mathrm{d}}^{-2} + \xi^{-2}$ with Eq. (24b) for δ_{d} and Eq. (25b) for ξ. As mentioned below Eq. (25), a mean-field description is not adequate for excluded-volume chains in a good solvent. In dilute solutions the radius of gyration scales as $R \sim N^{\nu}$, where ν is the Flory exponent: $\nu = 0.5$ in a theta solvent and $\nu = 0.588$ (Refs. 27 and 28) in a good solvent. In semidilute solutions we have $\xi \sim \varphi^{-\gamma}$, where the exponent γ is coupled to ν through $1/\gamma + 1/\nu = 3$.[21,27] Hence, $\gamma = 1$ in a theta solvent and $\gamma = 0.77$ in a good solvent. In order to apply the inverse-square relation of Eq. (26b), which is still a good approximation for excluded-volume chains,[21] we need also the prefactors. For a theta solvent $\delta_{\mathrm{d}} = 1.13R$ (Eq. (24b)) and $\xi = 0.658(\varphi^{\mathrm{b}})^{-1}$ (Eq. (25b)). For good solvents the result is

$$\delta_{\mathrm{d}} = 1.07R \quad \xi = 0.48\mathrm{v}^{-0.22}(\varphi^{\mathrm{b}})^{-0.77}. \tag{28}$$

The factor 1.07 for δ_{d} was found by Hanke *et al.*,[29] the expression for ξ is an estimate from Refs. 21 and 30 in which the simulation results by Louis *et al.*[31] were incorporated; these authors showed that also for excluded-volume chains a $\tanh^2$ density profile is adequate. Hence, the equation $\rho = \tanh^2[(z + p)/\delta]$ with δ given by Eq. (26b) plus 28 and p by Eq. (26c) is expected to be a good approximation for excluded-volume chains.[21] A check of this prediction for a wide range of variables is not easy, because excluded-volume profiles are far less available than SCF profiles.

VI. ADSORPTION RESULTS

A. Adsorption from semidilute solutions

For adsorption from semidilute solutions Eqs. (16) (with $\varepsilon = 0$), (17) and (18) still apply. Consequently, the same differential equations (Eq. (B2)) occur as for depletion. The difference is that now $g(z) > 1$, whereas for depletion g is below unity. As a result the tanh form of Eq. (25a) becomes a coth. As shown in Appendix B the approximate solutions are

$$g = \begin{cases} \coth\dfrac{z+p}{\xi} & good \\ \sqrt{\coth\dfrac{z+p}{\xi}} & theta \end{cases}, \tag{29a}$$

$$\xi = \begin{cases} \dfrac{1}{\sqrt{3\mathrm{v}\varphi^{\mathrm{b}}}} & good \\ \dfrac{1}{2\varphi^{\mathrm{b}}} & theta \end{cases}, \tag{29b}$$

$$p = \begin{cases} \dfrac{1}{\sqrt{3\mathrm{v}\varphi_0}} & good \\ \dfrac{1}{2\varphi_0} & theta \end{cases}. \tag{29c}$$

The value of the decay length ξ (Eq. (29b)) for a good solvent is the same as in Eq. (25b) for depletion; for a theta solvent there is a small difference in the numerical prefactor. The shift (proximal length) p is directly related to the train density φ_0. Equation (29c) was obtained using $\varphi_0 = \varphi^{\mathrm{b}} g_0^2$ with $\coth(p/\xi) = \xi/p$ for g_0 in Eq. (29a), which is valid as long as p/ξ, which equals $\sqrt{\varphi^{\mathrm{b}}/\varphi_0}$ (good solvent) or $\varphi^{\mathrm{b}}/\varphi_0$ (theta solvent), is small. In Sec. VI C we shall relate φ_0 and p to c and χ_s. Unlike for depletion, p cannot be zero, as this would lead to $g_0 = \infty$ and $\varphi_0 = \infty$. For strong adsorption ($\varphi_0 \approx 1$) the proximal length has a minimum value $p = 1/\sqrt{3\mathrm{v}}$ for good solvents and $p = 1/2$ for a theta solvent.

B. Adsorption from dilute solutions

We first define what we mean with dilute solutions. Typically, a polymer adsorption isotherm (e.g., the train density φ_0 as a function of φ^{b}) is characterized by a Henry region where φ_0 is proportional to φ^{b}, and a plateau region where φ_0 is of order unity and nearly independent of φ^{b}. The crossover between the two regimes occurs at $\varphi^{\mathrm{b}} = \varphi^* = \exp(-c^2R^2)$,[22] which under most conditions is an extremely small concentration. For example, for $N = 100$ and $\chi_s = -1$ it is $\varphi^* \approx 10^{-20}$; for higher N it is even lower. In this paper we do not discuss the Henry regime; we refer to earlier papers.[22] We restrict ourselves to the plateau region $\varphi^* < \varphi^{\mathrm{b}} < \varphi_{\mathrm{ov}}$, where φ_{ov} is the overlap concentration separating the dilute and semidilute regimes.

A full GSA solution for the dilute regime which includes trains and loops, tails, and free chains is rather complicated.[22] Here we present a simplified treatment which neglects tails and free chains; such a treatment is sufficient for describing the inner layer structure. Then the ground-state function g describes only loops (with $g_0 = g(0)$ accounting for trains). Consequently, the relation $\varphi = \varphi^{\mathrm{b}} g^2$ with $g = 1$ in the bulk solution no longer holds, since the loop concentration vanishes in the bulk solution. Following Ref. 22 we use $\varphi = g^2$, where φ and g refer only to loops (and trains for $z = 0$); both φ and g are zero for $z = \infty$. Now in the GS equation (Eq. (16)) the parameter ε is nonzero. The composition law (Eq. (7), again without the factor e^{u_z}) takes the form $\varphi \approx \varphi^{\mathrm{b}} g^2 e^{\varepsilon N}$ or, with $\varphi = g^2$, $\varepsilon \approx N^{-1}\ln(1/\varphi^{\mathrm{b}})$. As shown in Ref. 22 a slightly better approximation is $\varepsilon = N^{-1}\ln(\varphi_0/\varphi^{\mathrm{b}})$, or

$$\varepsilon = \frac{\ln(\varphi_0/\varphi^{\mathrm{b}})}{N} = \frac{1}{6d^2}, \tag{30a}$$

$$d = \frac{R}{\sqrt{\ln(\varphi_0/\varphi^{\mathrm{b}})}}, \tag{30b}$$

where d is the *distal length* characterizing the (exponential) decay of the loop segment concentration in the periphery of the adsorbed layer: in the distal region ($u = 0$) Eq. (16) reads $\mathrm{d}^2 g/\mathrm{d}(z/d)^2 = g$, with solution $g \sim e^{-z/d}$. The value of d is of order R, but it is lower by a factor $\sqrt{\ln(\varphi_0/\varphi^{\mathrm{b}})}$, which for $\varphi_0 \approx 1$ is 2.6 for $\varphi^{\mathrm{b}} = 10^{-3}$ and 4.6 for $\varphi^{\mathrm{b}} = 10^{-9}$.

We substitute $\varepsilon = 1/6d^2$ into the GS equation (Eq. (16)). For the field we have Eq. (17), in which we neglect φ^{b}: $u = \mathrm{v}\varphi = \mathrm{v}g^2$ for good solvents and $u = \varphi^2/2 = g^4/2$ for a theta solvent. This gives two differential equations (Eq. (B8)), which may be solved (Eq. (B9)) to give

$$g = \begin{cases} \dfrac{1}{d\sqrt{3\mathrm{v}}\sinh\frac{z+p}{d}} & good \\ \dfrac{1}{\sqrt{d\sinh\frac{2(z+p)}{d}}} & theta \end{cases}, \tag{31a}$$

$$p = \begin{cases} \dfrac{1}{\sqrt{3\mathrm{v}\varphi_0}} & good \\ \dfrac{1}{2\varphi_0} & theta \end{cases}. \tag{31b}$$

The relation $p(\varphi_0)$ in Eq. (31b) was found from $\varphi_0 = g_0^2$, using $\sinh(p/d) = p/d$ for g_0 in Eq. (31a). It is surprising that this relation is the same as in the semidilute regime (Eq. (29c)), despite the greatly different forms of the ground-state function g and the different relation between φ and g. The reason is that, for small z, $g \sim (z+p)^{-1}$ in a good solvent for both dilute and semidilute concentrations; for a theta solvent $g \sim (z+p)^{-1/2}$ in both cases. This relation $p(\varphi_0)$ is independent of the distal (decay) length of the profile (ξ for the semidilute regime, d for dilute solutions). The proximal length p is determined by short-range segment-surface interactions, and is thus related to φ_0 (or χ_s, see Sec. VI C); as in Eq. (29c) p has a minimum value $p = 1/\sqrt{3\mathrm{v}}$ for good solvents and $p = 1/2$ for a theta solvent.

In Sec. V A (Eq. (26)) we were able to find, for depletion, a good approximation for the intermediate concentration regime, thereby connecting the dilute and semidilute limits. For the adsorption case such a generalization is, so far, not

available. The adsorption problem is intrinsically more difficult than the relatively simple depletion case. However, the relation $p(\varphi_0)$ is independent of the concentration regime, and is therefore expected to be a good approximation for any concentration. In Sec. VI C we shall see that also the relation $c(\chi_s)$ does not depend on the concentration.

C. The relations $c(\chi_s)$ and $\varphi_0(\chi_s)$ for adsorption

We first consider briefly ideal chains for which we do not need GSA; we then use the full form of Eq. (20a) in terms of $G(z, N)$. For an ideal adsorbing chain Eq. (11) reduces to $G(z, N) = 2e^{Nc^2/6}e^{cz}$, where c is negative. The ratios occurring in Eq. (20a) are $G(0, N+1)/G(0, N) = e^{c^2/6}$ and $G(1, N)/G(0, N) = e^c$; we see that we now have to differentiate between N and $N+1$. Substituting these ratios into Eq. (20a) with $6e^{\mu_0} = 5e^{\Delta\chi_s}$ leads to

$$\Delta\chi_s = \ln\frac{4+e^c}{5} - \frac{c^2}{6}. \tag{32}$$

Also this equation was derived before for a single ideal end-grafted chain.[32] It gives $c = 5\Delta\chi_s$ for small negative $\Delta\chi_s$, which is the same result as for depletion (Eq. (22)). For high negative $\Delta\chi_s$, c decreases as $c^2 = -6\Delta\chi_s$ or $c = -\sqrt{-6\Delta\chi_s}$.

For chains consisting of finite-size segments, this unlimited decrease is not realistic as the factor $1-\varphi_0$ in Eq. (23) is important (and even dominates) for strong adsorption. In Eq. (23) we need the relation between φ_0 and c. This we obtain from $c = g_1/g_0 - 1$ (Eq. (19)), where we use the linearized forms of g_1 and g_0. From Eq. (29a) (semidilute) and Eq. (31a) (dilute) we find the *same* $c(p)$ or $c(\varphi_0)$ for both concentration regimes:

$$c = \begin{cases} \dfrac{1}{1+1/p} - 1 = \dfrac{1}{1+\sqrt{3\mathrm{v}\varphi_0}} - 1 & good \\ \dfrac{1}{\sqrt{1+1/p}} - 1 = \dfrac{1}{\sqrt{1+2\varphi_0}} - 1 & theta \end{cases}. \tag{33}$$

In the second form we inserted $p(\varphi_0)$ as given in Eqs. (29c) and (31b). Combining Eq. (23) for $\Delta\chi_s(c,\varphi_0)$ and Eq. (33) for $c(\varphi_0)$ we find either $\Delta\chi_s(\varphi_0)$ or $\Delta\chi_s(c)$. The first form is

$$5e^{\Delta\chi_s} = \begin{cases} (1-\varphi_0)\left(4+\dfrac{1}{1+\sqrt{3\mathrm{v}\varphi_0}}\right)\exp\left[\dfrac{\varphi_0}{6}(1-\mathrm{v})\left(4+\dfrac{1}{(1+\sqrt{3\mathrm{v}\varphi_0})^2}\right)\right] & good \\ (1-\varphi_0)\left(4+\dfrac{1}{\sqrt{1+2\varphi_0}}\right)\exp\left[\dfrac{\varphi_0}{6}\left(4+\dfrac{1}{1+2\varphi_0}\right)\right] & theta \end{cases} \tag{34}$$

whereas the second form is

$$5e^{\Delta\chi_s} = \begin{cases} \left(1-\dfrac{1}{3\mathrm{v}}\dfrac{c^2}{(1+c)^2}\right)(5+c)\exp\left[\dfrac{1/\mathrm{v}-1}{18}c^2\left(1+\dfrac{4}{(1+c)^2}\right)\right] & good \\ \left(1+\dfrac{c}{2}\dfrac{2+c}{(1+c)^2}\right)(5+c)\exp\left[\dfrac{-c(2+c)}{12}\left(1+\dfrac{4}{(1+c)^2}\right)\right] & theta \end{cases}. \tag{35}$$

We first check Eq. (34) against SCF. The symbols in Fig. 6 show numerical SCF data $\varphi_0(\Delta\chi_s)$ for $N = 1000$, $\varphi^b = 10^{-6}$, and five solvencies. The solid curves in Fig. 6 are the analytical results of Eq. (34). The agreement between numerical data and analytics in Fig. 6 is nearly quantitative for all solvencies.

The symbols in Fig. 6 are for $\varphi^b = 10^{-6}$ (dilute), but the numerical data for $\varphi^b = 10^{-2}$ (semidilute) are nearly the same, and they are also virtually independent of N. As discussed above, the analytical results do not depend on concentration: despite the different ground-state functions in the dilute regime (inverse sinh or its square root) and semidilute regime (coth or its square root) the expression for the train density (Eq. (34)) is the same (and independent of chain length).

Figure 7 shows the results for $c(\Delta\chi_s)$. Symbols are the numerical data from $c = G_1/G_0 - 1$, with for the G's the numerical end-point concentrations, as used in Fig. 3 for depletion. The solid curves are the theoretical adsorption branches from Eq. (35), for five solvencies. The dashed (steep) curve is the result for ideal chains (Eq. (32)), the dotted (even steeper) line is $c = 5\Delta\chi_s$ around the critical point. Very close to the critical point the GSA results coincide with those for ideal chains, but for $\Delta\chi_s$ as low as -0.05 the volume filling becomes important and the GSA curves start to level off. At high negative $\Delta\chi_s$, c saturates, both for GSA and for SCF. The SCF data are rather close to those predicted by our GSA treatment for finite-volume chains, with limiting values ranging from -0.66 (SCF) or $1/(1+\sqrt{3}) - 1 = -0.63$ (GSA) at $\chi = 0$ to -0.44 (SCF) or $1/\sqrt{3} - 1 = -0.42$ (GSA) at $\chi = 0.5$. For $\chi = 0.4$ and 0.45 the theoretical c is somewhat too high.

One may wonder why for $\varphi_0(\Delta\chi_s)$ in Fig. 6 there is nearly quantitative agreement between GSA and SCF, whereas for $c(\Delta\chi_s)$ in Fig. 7 deviations occur. The reason is that φ_0 is dominated by "average segments" (end segments contribute only slightly to φ_0), for which GSA is appropriate. The c parameter displayed in Fig. 7 is related to

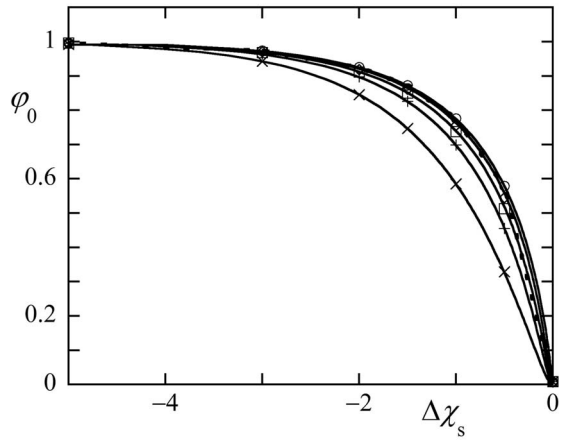

FIG. 6. Train density φ_0 as a function of $\Delta\chi_s$ in the adsorption regime, for $N = 1000$, $\varphi^b = 10^{-6}$, and five solvencies. Symbols are the SCF data for $\chi = 0$ (crosses), 0.3 (plusses), 0.4 (squares), 0.45 (diamonds), and 0.5 (circles). Curves are the analytical results of Eq. (34).

the end-point distribution, for which the GSA description is less accurate because end segments are treated as "middle" segments.

The most important conclusion from Fig. 7 is that due to volume filling the inverse extrapolation length reaches an lower limit $c \approx -0.5$, depending slightly on solvency: $c = 1/(1 + \sqrt{3v}) - 1$ for good solvents, $c = 1/\sqrt{3} - 1$ for a theta solvent.

Finally, we note that, like in Figs. 3 and 6, there is essentially no effect of the chain length or the bulk solution concentration in Fig. 7 (not shown). In the GSA treatment the result does not depend on N or φ^b, and also in the numerical SCF data there is hardly any difference in G_1/G_0 between long and short chains or between $\varphi^b = 10^{-6}$ (dilute) and $\varphi^b = 10^{-2}$ (semidilute).

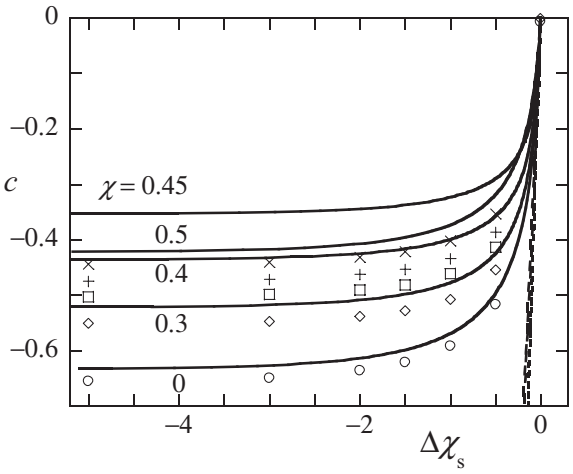

FIG. 7. Theoretical and numerical results for the inverse extrapolation length c as a function of $\Delta\chi_s$ for adsorption. Symbols are the numerical SCF data for $N = 1000$, $\varphi^b = 10^{-6}$, and five solvencies: $\chi = 0$ (circles), 0.3 (diamonds), 0.4 (squares), 0.45 (plusses), and 0.5 (crosses). The solid curves are theoretical GSA from Eq. (35). The dotted (steepest) line is $c = 5\Delta\chi_s$, the dashed curve (which in this range is close to $c = 5\Delta\chi_s$) is Eq. (32) for ideal chains.

D. GSA and SCF adsorption profiles

In Fig. 5 we showed GSA concentration profiles for depletion, and found excellent agreement with SCF. For adsorption we can also make such a comparison, but we expect larger deviations due to the various approximations made. With our present simplification (neglect of tails) it makes no sense to make detailed comparisons for the outer region of the adsorbed layer where tails dominate; such a comparison was made before[22] in a more involved treatment where also tails were accounted for. However, within our approximation we may consider the inner part of the profile, where tails contribute only slightly.

Figure 8 shows two sets of concentration profiles for $N = 5000$, for a dilute concentration ($\varphi^b = 0.001$) where Eq. (31) should apply (Fig. 8(a)) and for a semidilute concentration ($\varphi^b = 0.05$) described by Eq. (29) (Fig. 8(b)). The train volume fraction was chosen as $\varphi_0 = 0.6$, which fixes the proximal length p and the distal length d, see Eqs. (29c) and (30b). In each diagram results for four solvencies are shown, in the range $\chi = 0$ to $\chi = 0.5$. The solid curves give the GSA predictions, which start at 0.6 by definition. The symbols in Fig. 8 are SCF results, where χ_s was computed from Eq. (34) with $\varphi_0 = 0.6$. In Fig. 8(a) we plotted only the loop contribution (which goes to zero), in Fig. 8(b) the symbols refer to the overall profile (which goes to φ^b). Indeed, the numerical φ_0 is very close to 0.6, as expected on the basis of Fig. 6. For a good solvent the numerical SCF and analytical GSA profiles are in good agreement, although for $z > 0$ GSA gives a slight underestimation (which is most pronounced for $z = 1$).

The reason for this deviation is clear. For train segments ($z = 0$) we included the factor e^{u_0} (accounting for volume filling and non-local effect) through the boundary condition. However, the factor e^{u_z} for $z > 0$ is still absent in our GSA treatment: for these layers volume filling and non-local effect are not taken into account. Nevertheless, there is good agreement between SCF and GSA for good solvents. For a theta solvent the agreement is fair, but the deviations are stronger, for reasons discussed at length in Ref. 22. Anyhow, even for a theta solvent GSA gives a reasonable (though not perfect) description of the SCF data.

In Fig. 8(a) we plotted only the "dilute" GSA curves based upon Eq. (31a). However, there is for this dilute concentration hardly any difference with "semidilute" (Eq. (29a)); we did not show this in Fig. 8(a) in order not to complicate the picture. Similarly, in Fig. 8(b) "dilute" GSA (Eq. (31a)) gives for the inner layers nearly the same result as the "semidilute" curves shown. Clearly, for the outer layers there is a difference because "dilute" goes to $\varphi_{loops} = 0$, whereas "semidilute" reaches $\varphi_{overall} = 0.05$.

E. Determination of the adsorption energy parameter from experiment

The adsorption energy parameter (either c or χ_s) plays a crucial role in the behavior of polymers at interfaces, so it would be of great interest to determine this parameter from experiment. Unfortunately, information in the literature is scarce.

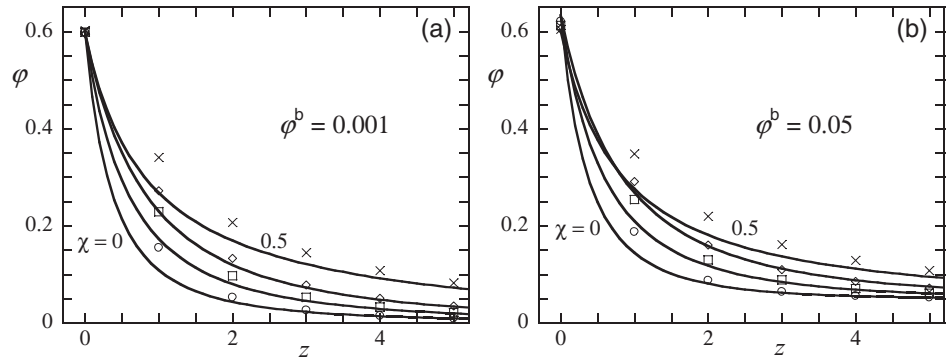

FIG. 8. Adsorption profiles $\varphi(z)$ for $N = 5000$ and $\varphi^b = 0.001$ (a) and $\varphi^b = 0.05$ (b), for four solvencies: $\chi = 0$ (circles), 0.3 (squares), 0.4 (diamonds), and 0.5 (crosses). Curves are analytical according to $\varphi = g^2$ with g from Eq. (31) (a) or according to $\varphi = \varphi^b g^2$ with g from Eq. (29) (b); in both cases φ_0 was set to 0.6, which fixes the parameters p and d. Symbols are SCF, with (a) "loops only" and (b) the overall profile (see text). The χ_s parameter needed for the SCF data was computed from Eq. (34) with $\varphi_0 = 0.6$.

For the adsorption regime, the most concise reports available are due to van der Beek *et al.*[33,34] These authors employed a displacement method, whereby an adsorbed polymer is desorbed by a more strongly adsorbing (monomeric) displacer. The displacer concentration φ_d at which the polymer is fully desorbed is a measure for the difference between the adsorption energy χ_s of the polymer and the adsorption energy χ_s^d of the displacer: the more negative χ_s^d, the lower φ_d. In order to determine χ_s of the polymer from an experimental value of φ_d, two conditions have to be met: the value of χ_s^d must be known (measured), and one needs a theoretical model relating χ_s, χ_s^d, and φ_d. In this procedure, there are many pitfalls; one of them is to account properly for solvency effects in the ternary mixture polymer/solvent/displacer. Nevertheless, useful data for several polymer/solvent systems on adsorbents such as silica and alumina have been obtained.

For the region of weak adsorption, some information is available from adsorption chromatography. Thrathnigg *et al.*[35] used ideal-chain theory to interpret elution data and extracted the c parameter (which in this region equals $5\Delta\chi_s$) by using homologous oligomers differing in chain length (e.g., chain length N and $N + 1$).

For the depletion regime, we are not aware of any attempts to determine the polymer-surface interaction parameter.

On the basis of the results presented in this paper, we make two additional suggestions to determine c or χ_s from experiment:

1. *Adsorption*. There are several methods to measure the train density φ_0 (and/or bound fraction) experimentally.[1,36] When φ_0 is known from experiment, Eq. (33) gives immediately the values of p and c, and Eq. (34) the value of $\Delta\chi_s$.
2. *Depletion*. There are a few situations where the concentration profile $\varphi(z)$ has been measured [e.g., Ref. 37]. No attempts have been made to interpret these measurements in terms of the polymer-surface interaction parameter. However, in principle these experiments provide the intercept φ_0 and (initial) slope $d\varphi/dz$. Using GSA ($\varphi \sim g^2$) we find the intercept I as $\varphi_0 \sim g_0^2$ and the slope S as $d\varphi/dz|_0 \sim 2g_0 dg/dz$. The ratio S/I equals $2g_0^{-1}dg/dz = 2c$ (Eq. (10) with $G = g$ because $\varepsilon = 0$) which provides an direct estimate for the interaction between polymer and surface. Alternatively, one could try to describe the experimental profile by $\rho = \tanh^2[(z + p)/\delta]$ and extract the two length scales p and δ from a curve fit. The c parameter is then obtained from Eq. (26c), which in turn gives χ_s (Eq. (22)).

VII. CONCLUDING REMARKS

We have shown in this paper that it is possible to connect the continuum and lattice descriptions for polymer adsorption and depletion, so that a rather complete picture with simple equations emerges. This is accomplished by combining the boundary conditions in the two models, which gives a relation between the inverse extrapolation length c as used in the continuum model and the lattice adsorption parameter χ_s.

For depletion the classical expression for the concentration profile is $\varphi(z) = \varphi^b \tanh^2(z/\delta)$, where δ is the depletion thickness. In dilute solutions $\delta = \delta_d$ is approximately equal to the radius of gyration R, which depends on the chain length N. In semidilute solutions δ equals the correlation length ξ, which is independent of N and is only a function of φ^b (and solvency χ). For intermediate concentrations δ is given by $\delta^{-2} = \delta_d^{-2} + \xi^{-2}$; it then depends on both R and φ^b (and again on χ). An accurate and simple equation for $\delta(R, \varphi^b, \chi)$ is now available, not only on the mean-field level but also for swollen excluded-volume chains.

The above expression assumes $\varphi(0) = \varphi_0 = 0$ at the surface, which restricts the validity to strong repulsion between segments and surface. Our generalization is to apply a shift p to z: we replace z by $z + p$, where p is the proximal length. It is determined by short-range interactions and is a known function of c and δ; for strong repulsion it equals the extrapolation length $1/c$. The inverse extrapolation length c is directly related to χ_s through $\Delta\chi_s = \ln(1 + c/5)$, independent of chain length, concentration, or solvency; in the depletion regime c and $\Delta\chi_s$ are positive. Here $\Delta\chi_s$ is defined with respect to the critical point, where both c and $\Delta\chi_s$ are zero. This

generalization, which is in quantitative agreement with exact SCF computations, is also valid for weak repulsion, down to the critical point $\Delta\chi_s = 0$. An experimental estimate of c (or $\Delta\chi_s$) could in principle be obtained from the ratio between intercept and (initial) slope of a measured concentration profile, or by determining p and δ from a curve fit.

Depletion results for real chains at finite concentrations follow from a generalization of the equations for ideal chains (or very dilute real chains). Also in the dilute limit two length scales occur: a depletion thickness δ_d which depends only on chain length, and a proximal length p which is a simple function of the interaction strength c (or χ_s) and δ_d. The recipe is straightforward: replace δ_d by the concentration-dependent δ, and the effect of concentration and solvency is automatically included.

For the adsorption regime, an analytical description of the concentration profile is more difficult because the occurrence of tails complicates the picture. However, we can obtain an accurate equation for the train density φ_0 as a function of $\Delta\chi_s$ (which is negative for adsorption). This relation, which now depends on solvency, is again in quantitative agreement with SCF results. Hence, it should be possible to determine $\Delta\chi_s$ from an experimental value of the train density.

The relation $\varphi_0(\Delta\chi_s)$ may be translated to $c(\Delta\chi_s)$. Here one should account for the finite size of a segment. In this respect the discrete train layer is analogous to the Stern layer as used in the classical description of the electrical double layer. The discrete feature of the train layer implies that the continuum boundary condition should also be used in a discrete form. The result is that for strong adsorption (high negative χ_s) the proximal length p has a minimum value ($1/\sqrt{3}$v for good solvents, 0.5 for a theta solvent), and that c assumes a minimum value $c \approx -0.5$ (depending slightly on solvency). This minimum of c is a direct consequence of the fact that the train volume fraction φ_0 can never exceed unity. An earlier description of $c(\Delta\chi_s)$ for ideal chains predicted that there is no lower limit: $c^2 \approx -6\Delta\chi_s$ for strong adsorption. The reason for this unrealistic behavior is obvious: the finite segment size and volume-filling constraint are absent for ideal chains. A realistic description for the adsorption regime necessarily requires taking into account the finite volume of a segment. That is one of the main results of our paper.

The relation between c and $\Delta\chi_s$ provides a quantitative connection between continuum and lattice theories, and enables the use of analytical continuum results to describe the depletion and adsorption of lattice chains at any chain length, concentration, and solvency. Some examples dealing with density profiles are given in the present paper. However, the treatment may be extended to chain stretching under the action of an external force. In a previous paper[16] we presented a fully analytical description of the mechanical desorption of a polymer chain, which includes the temperature dependence of the phase transitions. The analytical equations describe numerical results for flexible lattice chains down to oligomers (around 5 segments). Such an analysis is only possible when the mapping of lattice and continuum models, i.e., the relation $c(\Delta\chi_s)$, is available.

ACKNOWLEDGMENTS

A.M.S. acknowledges financial support through the Russian-German Grant No. N09-03091344 NNIO-a.

APPENDIX A: DENSITY PROFILE FOR IDEAL CHAINS

Eisenriegler's expression[25] for the density profile $\rho = \rho(\zeta,C)$ of an ideal chain next to a surface may be written as

$$\rho = 1 - \frac{1}{C^2}\left(Ae^{-\zeta^2} - Be^{-4\zeta^2}\right), \tag{A1}$$

where

$$A = [(2C\zeta+1)^2 + 2C^2 + 1]Y(\zeta) - 2Y(\zeta + C) - \frac{2C}{\sqrt{\pi}}(2C\zeta + 2), \tag{A2}$$

$$B = \left[2(2C\zeta+1)^2 + C^2 + 1\right]Y(2\zeta) + [4C\zeta + 2C^2 - 3]Y(2\zeta + C) - \frac{2C}{\sqrt{\pi}}(2C\zeta + 3). \tag{A3}$$

The function $Y(x)$ equals $e^{x^2}\mathrm{erfc}(x)$ (Eq. (12)). For $\zeta = 0$ we find $\rho_0 = \rho(\zeta = 0)$ as

$$\rho_0 = \left(2 - \frac{1}{C^2}\right)Y(C) - \frac{2}{\sqrt{\pi}C} + \frac{1}{C^2}. \tag{A4}$$

For strong repulsion (large C) $Y(C) \approx 1/(C\sqrt{\pi})$ and $\rho_0 \approx 1/C^2$ is small, for $C \to 0$ we have $Y(x) \approx 1 - 2C/\sqrt{\pi} + C^2$ and $\rho_0 \approx 1 - 4C/\sqrt{\pi}$ is close to 1.

Earlier[20] we showed that for strong repulsion the overall density profile ρ is very close to the distribution ρ_m of the middle segment, which may be written as

$$\rho_m = g_m^2 \quad g_m = \mathrm{erf}(\zeta\sqrt{2}) \approx \tanh(\zeta\sqrt{\pi}). \tag{A5}$$

Hence, g_m differs from the end-point distribution $g_e = G = \mathrm{erf}\,\zeta$ by a factor $\sqrt{2}$ in the argument.

This factor $\sqrt{2}$ suggests that we could find a simplification of the complicated Eqs. (A1)–(A3) by writing $\rho = G^2(\zeta\sqrt{2}, C/\sqrt{2})$, where $G(\zeta,C)$ is given by Eq. (11). This leads to

$$\rho = g^2 \quad g = \mathrm{erf}(\zeta\sqrt{2}) + e^{-2\zeta^2}Y(\zeta\sqrt{2} + C/\sqrt{2}), \tag{A6}$$

which is indeed a good approximation for the depletion regime. We obtain also a simpler expression for ρ_0:

$$\rho_0 = Y^2(C/\sqrt{2}), \tag{A7}$$

which is in close agreement with the more complicated Eq. (A4).

We now also find a justification of Eq. (13) for the end-point distribution. For strong repulsion this is $G = \mathrm{erf}(\zeta)$, which may be transformed to the tanh form as used in Eq. (A5): $G \approx g_e$ with

$$g_e = \tanh(\zeta\sqrt{\pi/2}). \tag{A8}$$

In Eq. (13) we also accounted for weaker repulsion by applying a shift atanh$Y(C)$ to $\zeta\sqrt{\pi/2}$ as explained in the main text.

APPENDIX B: GSA DESCRIPTION FOR DEPLETION AND ADSORPTION

1. Semidilute solutions

Equation (18) may be written as

$$u = \begin{cases} \xi^{-2}(g^2-1)/3 & \xi = 1/\sqrt{3\mathrm{v}\varphi^b} \quad good \\ \xi_t^{-2}(g^4-1)/3 & \xi_t = \sqrt{2/3}/\varphi^b \quad theta \end{cases}, \tag{B1}$$

where ξ is the semidilute correlation length. For a theta solvent we use the symbol ξ_t; below we shall use a length scale ξ for a theta solvent which differs from ξ_t by a numerical factor. We define a scaled spatial coordinate $x = z/\xi$ or $x = z/\xi_t$. Substituting Eq. (B1) and $\varepsilon = 0$ into Eq. (16) gives the following differential equations:

$$\frac{\mathrm{d}^2 g}{\mathrm{d}x^2} = \begin{cases} 2(g^3-g) & good \\ 2(g^5-g) & theta \end{cases}. \tag{B2}$$

The solution of the good-solvent form of Eq. (B2) is

$$g = \begin{cases} \tanh x & depletion \\ \coth x & adsorption \end{cases}. \tag{B3}$$

These forms were used in Eqs. (25a) (depletion) and (29a) (adsorption from a good solvent). Clearly, we may apply a shift s (where s is a constant) to x: when tanh x satisfies Eq. (B2), tanh$(x + s)$ is a solution as well. In Eqs. (25a) and (29a) we used $s = p/\xi$, with p the proximal length.

As shown in Ref. 20 the solution of the second form of Eq. (B2) for theta solvents is

$$x\sqrt{8} = \mathrm{atanh}\frac{g\sqrt{6+3g^2}}{1+2g^2} + C$$

$$C = \begin{cases} 0 & depletion \\ -\mathrm{atanh}\dfrac{\sqrt{3}}{2} & adsorption \end{cases}, \tag{B4}$$

which gives x as a function of g. The value of the integration constant C ensures that $g(x = 0) = 0$ for depletion and $g(x = 0) = \infty$ for adsorption. Inversion of Eq. (B4) with $C = 0$ gives for depletion in a theta solvent[20]

$$g^2 = \frac{\cosh(x\sqrt{8})-1}{\cosh(x\sqrt{8})+2} \approx \tanh^2\left(\frac{x}{a}\right)$$

$$a = \sqrt{\frac{3}{2}}\mathrm{atanh}\frac{1}{\sqrt{3}} = 0.806. \tag{B5}$$

The approximation $g = \tanh(x/a)$ is very accurate (within 1%). The constant a was obtained by demanding the same integral over $1 - g^2$,[20] which is equivalent to the same depletion thickness for the two forms of g^2. We now define $\xi = a\xi_t$ and use the simple form $g = \tanh(z/\xi)$ with $\xi = \mathrm{atanh}(1/\sqrt{3})/\varphi^b = 0.658/\varphi^b$, as in Eq. (25b). Again, we may apply a shift p to z.

For adsorption from a theta solvent we have to invert Eq. (B4) with $C = -\mathrm{atanh}(\sqrt{3}/2)$; this requires solving a quartic equation in g. The solution is

$$g^2 = \frac{f(t)}{t} \approx \coth\left(x\sqrt{\frac{8}{3}}\right) \qquad t = \frac{\tanh(x\sqrt{8})}{\sqrt{3}}$$

$$f(t) = \frac{(2+t)^2 - 2 + (2+3t)\sqrt{1-3t^2}}{4+7t} \tag{B6}$$

The important part is $g^2 \sim 1/t = \sqrt{3}\coth(x\sqrt{8})$ because the correction factor $f(t)$ depends only weakly on t, varying from $f(0) = 1$ to $f(1/\sqrt{3}) = 1/\sqrt{3} = 0.577$. Surprisingly, the approximation $g^2 = \coth(x\sqrt{8/3})$ whereby the prefactor $1/\sqrt{3}$ is transferred *into* the argument is very accurate, underestimating the full solution by less than 1%. This approximation was used in Eq. (29a), in the form $g^2 = \coth(z/\xi)$ with $\xi = \sqrt{3/8}\xi_t = (1/2)/\varphi^b$. Again a shift p was applied in Eq. (29a). For adsorption p must be nonzero (unlike for depletion) because otherwise $g(0) = g_0$ would become infinite.

2. Adsorption from dilute solutions

In dilute solutions we do not consider the overall profile (including free chains) but only the adsorbed part. A full GSA treatment[22] requires taking into account train-loop and tail contributions, which can be described by *two* eigenfunctions g and f: the train-loop part is proportional to g^2 and the tail part is proportional to the product gf. Here we are mainly interested in the inner layer structure, where tails are negligible. Then we need only the function g for trains and loops, with $\varphi \approx g^2$.

For large z (the distal region) $u = 0$ and Eq. (16) reads $\mathrm{d}^2 g/\mathrm{d}z^2 = 6\varepsilon g = d^{-2} g$, where we used $6\varepsilon = d^{-2}$ (Eq. (30a)). Hence, in this region $g \sim \mathrm{e}^{-z/d}$ for loops decays exponentially, with a decay length d given by Eq. (30b). For smaller z the field is nonzero: $\mathrm{d}^2 g/\mathrm{d}z^2 = (d^{-2} + u)g$, with

$$u = \begin{cases} \mathrm{v}g^2 & good \\ g^4/2 & theta \end{cases}, \tag{B7}$$

which is Eq. (17) with $\varphi = g^2$ and $\varphi^b \approx 0$. We use again a scaled spatial coordinate $x = z/d$ and introduce a renormalized eigenfunction h so that the GS equation (Eq. (16)) becomes

$$\frac{\mathrm{d}^2 h}{\mathrm{d}x^2} = \begin{cases} h + 2h^3 & h = gd\sqrt{3\mathrm{v}} \quad good \\ h + 3h^5 & h = g\sqrt{d} \quad theta \end{cases}. \tag{B8}$$

The solution is

$$h = \begin{cases} \dfrac{1}{\sinh x} \\ \dfrac{1}{\sqrt{\sinh(2x)}} \end{cases} \qquad g = \begin{cases} \dfrac{1}{d\sqrt{3\mathrm{v}}\sinh x} & good \\ \dfrac{1}{\sqrt{d\sinh(2x)}} & theta \end{cases}, \tag{B9}$$

which is Eq. (31a). As before, in Eq. (31a) we applied a shift p to z; again p cannot be zero.

Equation (B9) with $x = (z + p)/d$ is generally valid for loops, both in the Henry region (where φ_0 is proportional to φ^{b}) and in the plateau region of the adsorption isotherm (where φ_0 is of order unity and nearly independent of φ^{b}). As shown in Ref. 22, we need two equations to determine p and d: conservation of end-points and lattice boundary condition. It turns out that the crossover between Henry and plateau regions is situated at $\varphi^{\mathrm{b}} = \varphi* = e^{-c^2R^2}$, which is an extremely small concentration under most conditions. For $\varphi^{\mathrm{b}} < \varphi^*$ (Henry region) $p > d$ and then the parameter p is irrelevant and does not enter the equations: the only length scale is $d = -1/c$, which leads to $\varphi_0 = \varphi^{\mathrm{b}}/\varphi^*$ and $\varphi(z) = \varphi_0 e^{-2z/d} = \varphi_0 e^{2zc}$ in this regime. In the main text we discussed only the plateau regime ($p < d$), where two length scales occur: a proximal length p (which depends on c or χ_s) and a distal length of order R: $d = R/\sqrt{\ln(\varphi_0/\varphi^{\mathrm{b}})}$ (Eq. (30b)).

[1] G. J. Fleer, M. A. Cohen Stuart, J. M. H. M. Scheutjens, T. Cosgrove, and B. Vincent, *Polymers at Interfaces* (Chapman and Hall, London, 1993).
[2] G. J. Fleer, M. A. Cohen Stuart, and F. A. M. Leermakers, "Effect of polymers on the interaction between colloidal particles" in *Fundamentals of Interface and Colloid Science, Soft Colloids*, edited by J. Lyklema (Elsevier, Amsterdam, 2005), Vol. V, Chap. 1, pp. 1.1–1.94.
[3] R. J. Hunter, *Foundations of Colloid Science*, 2nd ed. (Oxford University Press, Oxford, 2001).
[4] T. Sakaue, E. Raphael, P. G. De Gennes, and F. Brochard-Wyart, Europhys. Lett. **72**, 8 (2005).
[5] G. Gregoriadis, Trends Biotechnol. **13**, 527 (1995).
[6] H. Pasch and B. Trathnigg, *HPLC of Polymers* (Springer-Verlag, Berlin, 1999).
[7] F. Pincet, E. Perez, and G. Belfort, Langmuir **11**, 1229 (1995).
[8] S. L. Levy and H. G. Craighead, Chem. Soc. Rev. **39**, 1133 (2010).
[9] P. J. Flory, *Principles of Polymer Chemistry* (Cornell University, Ithaca, NY, 1957).
[10] A. Silberberg, J. Chem. Phys. **48**, 2835 (1968).
[11] B. R. Postmus, F. A. M. Leermakers, and M. A. Cohen Stuart, Langmuir **24**, 6496 (2008).
[12] M. Charlaganov and F. A. M. Leermakers, J. Chem. Phys. **131**, 244115 (2009).
[13] S. F. Edwards, Proc. Phys. Soc. **85**, 613 (1965); **88**, 265 (1965).
[14] G. C. Gouy, J. Phys. **9**, 457 (1910); D. L. Chapman, Philos. Mag. **25**, 475 (1913).
[15] O. Stern, Z-Electrochem. **30**, 508 (1924).
[16] A. M. Skvortsov, L. I. Klushin, G. J. Fleer, and F. A. M. Leermakers, J. Chem. Phys. **132**, 064110 (2010).
[17] R. J. Rubin, J. Chem. Phys. **43**, 2392 (1965).
[18] A. A. Gorbunov and A. M. Skvortsov, Adv. Colloid Interface Sci. **62**, 31 (1995).
[19] P. G. De Gennes, *Scaling Concepts in Polymer Physics* (Cornell University, Ithaca, NY, 1979).
[20] G. J. Fleer, A. M. Skvortsov, and R. Tuinier, Macromolecules **36**, 7857 (2003).
[21] G. J. Fleer, A. M. Skvortsov, and R. Tuinier, Macromol. Theory Simul. **16**, 531 (2007).
[22] G. J. Fleer, J. van Male, and A. Johner, Macromolecules **32**, 825 (1999); **32**, 845 (1999).
[23] Y. Lepine and A. Caillé, Can. J. Phys. **56**, 403 (1978).
[24] E. Eisenriegler, K. Kremer, and K. Binder, J. Chem. Phys. **77**, 6296 (1982).
[25] E. Eisenriegler, J. Chem. Phys. **79**, 1052 (1983).
[26] M. Doi and S. F. Edwards, *The Theory of Polymer Dynamics* (Oxford University Press, Oxford, 1986).
[27] G. des Cloiseaux and G. Jannink, *Polymers in Solution* (Oxford University Press, Oxford, 1990).
[28] H. P. Hsu and P. Grassberger, J. Chem Phys. **120**, 2034 (2004).
[29] A. Hanke, E. Eisenriegler, and S. Dietrich, Phys. Rev. E **59**, 6853 (1999).
[30] G. J. Fleer and R. Tuinier, Adv. Colloid Interface Sci. **143**, 1 (2008).
[31] A. A. Louis, P. G. Bolhuis, and E. J. Meijer, J. Chem. Phys. **116**, 10547 (2002).
[32] A. A. Gorbunov, A. M. Skvortsov, J. van Male, and G. J. Fleer, J. Chem. Phys. **114**, 5366 (2001).
[33] G. P. van der Beek, M. A. Cohen Stuart, G. J. Fleer, and J. E. Hofman, Langmuir **5**, 1180 (1989).
[34] G. P. van der Beek, M. A. Cohen Stuart, G. J. Fleer, and J. E. Hofman, Macromolecules **24**, 6600 (1991).
[35] B. Thrathnigg, M. I. Malik, O. Jamelnik, and N. V. Cuong, Anal. Chem. Acta **604**, 39 (2007).
[36] M. A. Cohen Stuart, T. Cosgrove, and B. Vincent, Adv. Colloid Interface Sci. **24**, 143 (1986).
[37] D. Ausseré, H. Hervet, and F. J. Rondelez, Phys. Lett. **46**, L929 (1985).